DMO in arbitrary 3-D acquisition geometries

SP4.5

Gijs J.O. Vermeer; Shell Research Rijswijk, The Netherlands; Huub PGM. den Rooijen, Shell UK E&P; and Jan Douma, Nederlandse Aardolie Maatschappij

Summary

This paper provides a theory for the application of 3D dip moveout (DMO) to data with varying shot/receiver offsets and azimuths.

We derive a general expression for the DMO-corrected time of a plane, dipping event in a constant-velocity medium. Inspection of that expression shows that DMO can be applied successfully to 3D single-fold subsets of arbiirary 3D acquisition geometries, provided those subsets are sampled alias-free.

We illustrate this for the data of a cross-spread, the single-fold basic subset of the orthogonal geometry. In this data set the midpoints of the traces contributing to an output point fall along a hyperbola in the (x,y)-plane. The hyperbola contains exactly one shot/receiver pair that has illuminated the footpoint of the normal-incidence ray at the output point. This footpoint is found through DMO.

Correct sampling of the hyperbolas is difficult to achieve. Therefore, even in regularly sampled data sets, the result of 3D DMO for data with varying shot/receiver azimuths is usually suboptimal.

Introduction

The dip moveout (DMO) operator is intended to correct for reflection point smear of traces in the same midpoint gather. It was originally devised for pure 2D data, which are acquired with shots and receivers located on the same straight line. The extension to marine 3D was straightforward insofar as common offset gathers are also common azimuth gathers. But, as far as we know, no satisfactory theory has been published that justifies the application of the DMO process to more general 3D acquisition geometries, in which shot/receiver azimuths vary over all possible values. Despite this lack of a theoretical basis, 3D DMO is often applied to land seismic data with surprisingly good results. For instance, Forel and Gardner (1988) demonstrated that 3D DMO deals adequately with synthetic data having random azimuth variations. Similarly, Yao et al. (1993) used a physical model to show that the operation can handle wide azimuth data as well as narrow azimuth data. Those results and actual processing practice call for a theory of 3D DMO in arbitrary geometries.

A noteworthy feature of 2D DMO is that it "works" for single-fold common offset gathers. For each output point, every gather always contains a single trace which has illuminated the same point on the reflector as the normal-incidence trace for the output point (assuming dense sampling). All other traces in the gather either contribute to the zone of stationary phase around that trace, or cancel each other along the flanks of the output operator. In this paper we show that a similar process operates in other single-fold data sets,-particularly in the cross-spread, the single-fold basic subset of the orthogonal geometry (Vermeer, 1994).

On our way to this result we first derive a general expression for the time of a DMO-corrected event. This expression allows us to postulate a general criterion for successful 3D DMO in single-fold 3D data sets. Then we derive, for the cross-spread, the locus of midpoints that contribute to an output point. We prove that the single-fold cross-spread data are suitable for imaging with DMO. Finally, we make some remarks about other geometries and discuss some sampling-related problems. In our work we assume the reflectors have a constant dip in a constant velocity medium.

The time of a DMO-corrected event

Figure 1 illustrates the reflection point smear that DMO is supposed to correct. The shot/receiver pair (S,R) records a reflection from the depth point D which is posted at the midpoint M. The DMO-operation has to move the reflection to the normal-incidence point 0 and give it the normal-incidence time of 0. As the subsurface dip is unknown, DMO is an imaging process in which all traces that can contribute to a particular output point 0 are moved to that point after application of the DMO-correction. We call the collection of traces contributing to the output point a DMO panel.

If 3D DMO is to be successful in imaging an event, then (in analogy to 2D DMO) the DMO panel should meet three conditions:

- It should have a point of stationary phase.
- The DMO-corrected time in that point should be equal to the normal-incidence time for the output point.
- The DMO panel should contain a well-sampled collection of traces around the point of stationary phase.

We want to establish in this paper which single-fold data sets may produce DMO panels that satisfy these conditions.

To achieve this, we first compute the DMO-corrected time for a trace moved from M to 0 (Figure 2). Suppose the subsurface contains a dipping reflecting plane:

$$\{(x,y,z): n_x x + n_y y + n_z z - a = 0 \wedge \|n\| = 1\}, \qquad (1)$$

where
$n = (n_x, n_y, n_z)^T = (\sin\theta_0 \cos\varphi_0, \sin\theta_0 \sin\varphi_0, \cos\theta_0)^T$, and θ_0, φ_0 are reflector dip and azimuth. The normal-incidence reflection time in the origin 0 is

$$t_0 = 2a/c, \qquad (2)$$

where c is the constant propagation velocity.

We now consider a shot at (x_s, y_s) and a receiver at (x,, y_r) with corresponding midpoint (x_m, y_m) and half-off set $(h_x, h_y) = ((x_r - x_s)/2, (y_r - y_s)/2)$. The reflection traveltime is given by

$$t = \frac{2}{C}\left[(a - n_x x_m - n_y y_m)^2 - (n_x h_x + n_y h_y)^2 + h^2\right]^{1/2} \quad (3)$$

where $h := \sqrt{h_x^2 + h_y^2}$. Application of the NMO-correction with dip-independent velocity c leads to

$$t_n = \frac{2}{c}\left[(a - n_x x_m - n_y y_m)^2 - (n_x h_x + n_y h_y)^2\right]^{1/2} \quad (4)$$

As already indicated in Figure 2, the shot/receiver pair can only contribute to the DMO output in the origin if the shot/receiver segment passes through 0. We introduce r and φ: r is the distance from 0 to M ; $r > 0$ if 0 lies between M and S, and $r < 0$ if 0 lies between M and R; $|r| < h$. φ is the angle measured from positive x-axis to *OR*. Then, expressing x_m, y_m, h_x and h_y in terms of r, h and φ, and expressing n_x, n_y in terms of θ_0 and φ_0, we get

$$t_n = \frac{2}{c}\left[(a - r\sin\theta)^2 - h^2\sin^2\theta\right]^{1/2}. \quad (5)$$

Here θ is the apparent dip along azimuth φ, it is defined by $\sin\theta = \sin\theta_0 \cos(\varphi - \varphi_0)$.

The DMO-corrected time t_d is found by multiplying the NMO-corrected time t_n by the DMO-correction factor (Deregowski, 1982) :

$$t_d = t_n\sqrt{1 - \frac{r^2}{h^2}}. \quad (6)$$

Combining Eqs. 5 and 6 yields the DMO-corrected time at the output point:

$$t_d = \frac{2a}{c}\left[1 - \left(\frac{ar + (h^2 - r^2)\sin\theta}{ah}\right)^2\right]^{1/2} \quad (7)$$

Note that this formula is valid for arbitrary shot/receiver offsets and azimuths, the only requirement being that the output point lie on the shot/receiver segment. Eq. 7 shows that the DMO-corrected time at an output point for a plane, dipping event is always less than or equal to the true normal-incidence time at that point. The DMO-corrected time is equal to the normal-incidence time only if

$$ar + (h^2 - r^2)\sin\theta = 0. \quad (8)$$

In the case $\theta = 0$, the solution of Eq. 8 is $r = 0$, i.e., midpoint and normal-incidence point coincide for a horizontal reflector and also for shooting along strike. Otherwise, Eq. 8 can be written as $(h - r)(h + r) = d|r|$, where $d = a/|\sin\theta|$ (see Figure 1). This is exactly the same equation as that for a shot/receiver pair that has its reflection point at the footpoint of the normal-incidence ray at the output point. This equivalence expresses the property that DMO removes reflection-point dispersal (Deregowski, 1982).

Eq. 8 can be solved only if r has a sign opposite to that of sine. Therefore, in order for DMO to image the normal-incidence event for positive and negative dips, the DMO panel must contain traces on both sides of the output point.

Now we postulate that the main criterion for a successful 3D DMO in single-fold 3D subsets of arbitrary acquisition geometries is that the subsets should be alias-free. Alias-free sampling allows construction of DMO panels for each output point with the property that the midpoints of the traces in the DMO panel are distributed along a smooth curve passing through the output point. This curve is called the locus of contributing midpoints.

Basically, our criterion of alias-free sampling means that the spatial variables vary smoothly in the data set. This ensures that somewhere along the locus Eq. 8 is satisfied (the point of stationary phase), whereas elsewhere the DMO-corrected events follow a smoothly varying curve according to Eq. 7 (zone of stationary phase and flanks).

A formal proof of the suitability of certain 3D single-fold data sets for 3D DMO would include a description of allowable locations of the output point. Here we restrict ourselves to proving that Eq. 8 has a solution for the single-fold cross-spread.

Contributing traces in cross-spread

The cross-spread is a 3D single-fold data set consisting of all traces that have a shot line and an orthogonal receiver line in common. For the time being we consider the cross-spread as a continuous data set, i.e., shots and receivers can occupy any position along the acquisition lines.

The DMO panel at an output point 0 in a cross-spread consists of those traces whose shot/receiver segment passes through that point. Take any shot S along the shotline and connect it with 0 (Figure 3). The line SO intersects the receiver line at R. The corresponding midpoint M is a point on the locus of contributing midpoints, provided 0 lies between R and S, i.e., only midpoints in the same quadrant of the cross-spread as the output point can contribute to this point. Taking 0 as the origin of our coordinate system and (X,Y) as the centre of the cross-spread, we can describe the locus by the equation

$$(x_m - \frac{X}{2})(y_m - \frac{Y}{2}) = \frac{XY}{4}. \quad (9)$$

Hence, the DMO panel is formed by traces whose midpoints lie on an orthogonal hyperbola passing through 0, with asymptotes halfway between 0 and the shot and receiver lines.

Using Eq. 9, $X = \rho\cos\beta$, $Y = \rho\sin\beta$ and geometric relations (see Figure 3), one can parametrise r and h of a midpoint on the locus in terms of the shot/receiver azimuth φ:

$$r(\varphi) = \rho\,\frac{\sin(\beta + \varphi)}{\sin 2\varphi}, \quad (10)$$

$$h(\varphi) = \rho\,\frac{\sin(\beta - \varphi)}{\sin 2\varphi}. \quad (11)$$

The DMO-corrected time in the cross-spread

Eqs. 7, 10 and 11 together describe the time $t_d(\varphi)$ of the dipping event in the DMO panel. We rewrite Eq. 7 as:

$$t_d(\varphi) = t_0\sqrt{1 - \gamma^2(\varphi)}, \quad (12)$$

where

$$\gamma(\varphi) = \frac{ar + (h^2 - r^2)\sin\theta_0 \cos(\varphi - \varphi_0)}{ah}. \quad (13)$$

Substitution of the expressions for $r(\varphi)$ and $h(\varphi)$ into Eq. 13 gives

$$\gamma(\varphi) = \frac{-a\sin(\varphi+\beta) + \rho\sin 2\beta \sin\theta_0 \cos(\varphi - \varphi_0)}{a\sin(\varphi-\beta)}. \quad (14)$$

The stationary point φ_s of the DMO panel, defined by

$$\left.\frac{\partial t_d(\varphi)}{\partial\varphi}\right|_{\varphi=\varphi_s} = 0, \quad (15)$$

is attained for $\gamma(\varphi_s) = 0$, i.e., $t_d(\varphi_s) = t_0$. We find

$$\tan\varphi_s = -\frac{Y(a-2n_xX)}{X(a-2n_yY)} = -\frac{\sin\beta(a-2\rho\cos\beta\sin\theta_0\cos\varphi_0)}{\cos\beta(a-2\rho\sin\beta\sin\theta_0\sin\varphi_0)}. \quad (16)$$

This shows that there is a stationary point at $t = t_0$, which proves that the proper normal-incidence time can be found by the application of DMO to cross-spread data, provided the extent of the cross-spread is large enough. Note that there is only one stationary point for each output point.

Figure 4 shows some graphs computed along the locus of midpoints of contributing traces as a function of DMO shift r. These graphs describe the DMO operation in the orthogonal geometry.

Extension to other geometries

We have shown that the DMO operation can be applied successfully to single-fold cross-spread data in which the locus of contributing midpoints is an orthogonal hyperbola. Our derivations can be easily extended to geometries in which shot and receiver lines cross at arbitrary angles. Then the loci are oblique hyperbolas with asymptotes parallel to the acquisition lines.

In the parallel geometry the hyperbolas reduce to straight lines, provided the distance between shot and receiver lines is kept constant. Then DMO can operate in common offset gathers with constant shot/ receiver azimuth. However, our analysis does not cover DMO in wide multi source/multi streamer configurations, because no alias-free single-fold 3D subsets can be constructed for those geometries.

Not only oblique cross-spreads are suitable for DMO, in fact all 3D single-fold datasets with an areal distribution of midpoints are suitable for 3D DMO, provided they are alias-free. These datasets include 3D common shot and common receiver gathers as well as cross-spreads acquired with smooth rather than straight acquisition lines.

Sampling problems

Conventional DMO programs use output bins rather than output points. All traces with a shot/receiver segment that cross the output bin may contribute a DMO-corrected trace to that bin (depending on the. sampling along the shot/receiver segment). This is illustrated in Figure 5 for the cross-spread. In Figure 5a two hyperbolas are drawn, each of which is a locus of contributing midpoints for one corner of the bin. All midpoints which lie between the two hyperbolas have shot/receiver segments that pass through the bin; hence, they are potential contributors to the DMO panel for the bin. These midpoints are plotted in Figure 5b. Application of the DMO-correction to these traces leads to time jitter in the DMO panel.

An ideal DMO output can only be obtained if the locus of midpoints can be properly sampled. Unless the necessary sample points along the loci are derived from the existing sample points, DMO output will not be ideal. However, resampling to obtain new samples along each and every locus of contributing midpoints is a very expensive exercise. A good compromise is to use finer sampling of the midpoints in the cross-spread.

In marine data acquisition (with streamers) the DMO panels have to be equalised to correct for irregular sampling (Canning and Gardner, 1992; Beasley and Klotz, 1992). In land data acquisition (with the orthogonal geometry) it is not necessary to equalise DMO panels. Instead, regular alias-free cross-spreads should be acquired; alternatively, the cross-spreads should be regularised.

Conclusions

We derived an expression for constant-velocity DMO in arbitrary acquisition geometries. From this expression it follows that alias-free single-fold 3D data sets are suitable for 3D DMO, irrespective of the shot/receiver azimuths in the data set. We have proved this for the cross-spread, the basic subset of the orthogonal geometry.

Acknowledgements

We would like to thank Shell lnternationale Petroleum Maatschappij and Shell Research B.V. for permission to publish this paper. The suitability of cross-spreads for 3D DMO was first demonstrated by T. Padhi.

References

Beasley, C.J., and Klotz, R., 1992, Equalization of DMO for irregular spatial sampling: 62nd Ann. Internat. Mtg., Soc. Expl. Geophys., Expanded Abstracts, 970-973.

Canning, A., and Gardner, G.H.F., 1992, Feathering correction for 3-D marine data: 62nd Ann. Internat. Mtg., Soc. Expl. Geophys., Expanded Abstracts, 955-975.

Deregowski, S.M., 1982, Dip-moveout and reflection point dispersal: Geoph. Prosp., 30, 318-322.

Forel, D., and Gardner, G.H.F., 1988, A three-dimensional perspective on two-dimensional dip moveout: Geophysics, 53, 604-610.

Vermeer, G.J.O., 1994, 3D symmetric sampling: 64th Ann. Internat. Mtg., Soc. Expl. Geophys., Expanded Abstracts,.

Yao, P.C., Sekharan, K.K., and Ebrom, D., 1993, Data acquisition geometry and 3-D DMO: 63rd Ann. Internat. Mtg., Soc. Expl. Geophys., Expanded Abstracts, 552-554.

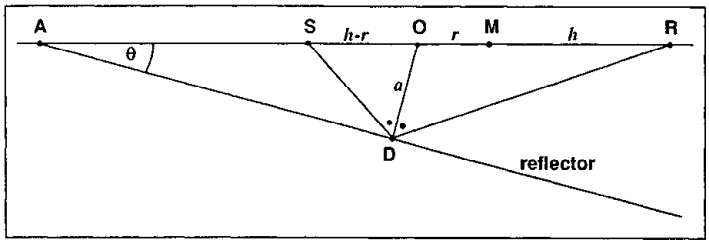

Figure 1 Geometry of plane dipping reflector. Putting d = OA and with OS : OR = SD : RD = AS : AR, it follows that $(h\text{-}r)(h+r)=dr$.

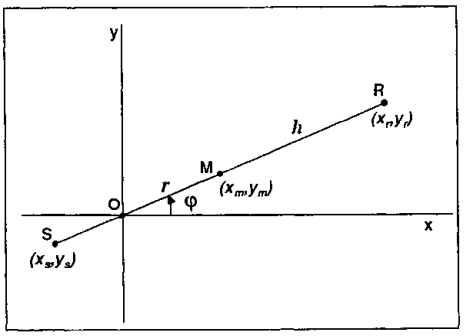

Figure 2 Contributing source-receiver pair for output point in the origin.

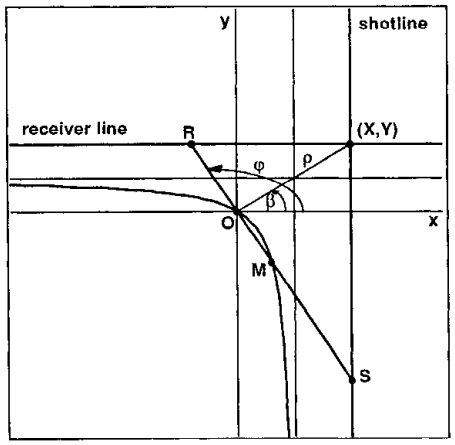

Figure 3 Orthogonal cross-spread acquisition geometry. Locus of contributing midpoints of an output point 0 is a hyperbola through 0.

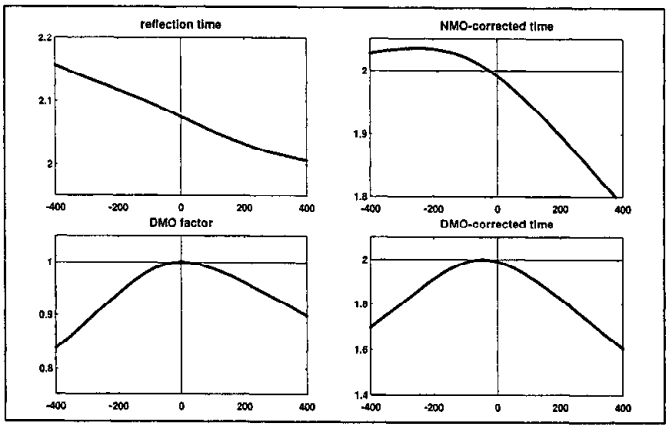

Figure 4 Graphs computed along locus of contributing midpoints for dipping reflector. Horizontal axis is (signed) distance r from midpoint to output point. *(Origin in centre of cross-spread, output pointX = 500 m,* Y = *300 m; reflector* $t_0 = 2$ s, $\theta_0 = 30°$, $\varphi_0 = 18°$)

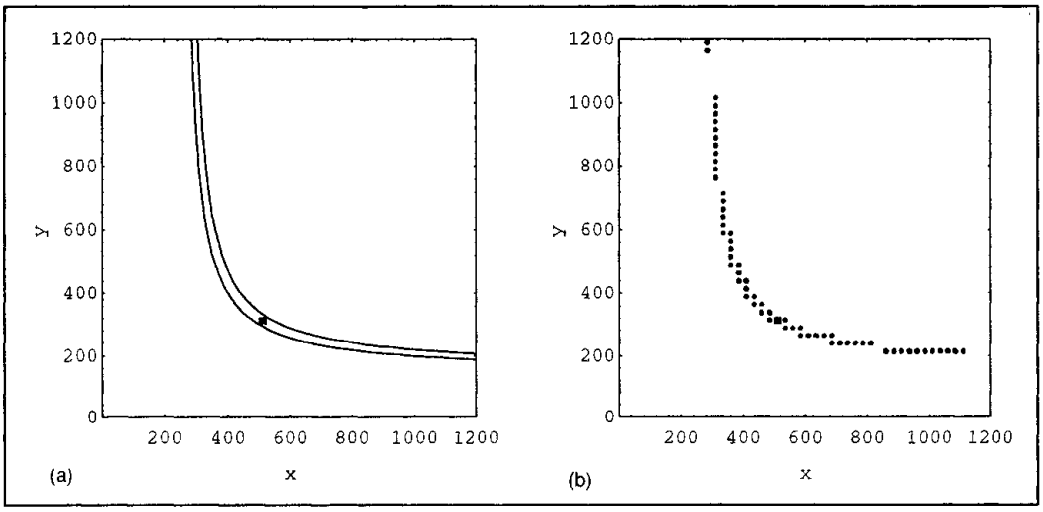

Figure 5 Loci of contributing midpoints for one output bin, represented by black square. (a) area between hyperbolas contains all midpoints contributing to bin; (b) actual input midpoints.